Kinetic Study and Modeling of the High Temperature CO_2 Capture by Na_2ZrO_3 Solid Sorbent

*Diana Barraza Jiménez, Daniel Lardizábal Gutiérrez, Virginia Collins Martínez and Alejandro López Ortiz**

Centro de Investigación en Materiales Avanzados S. C. Miguel de Cervantes 120, Complejo Industrial Chihuahua, Chihuahua, México 31109.
**Author to whom correspondence should be addressed, email:*
alejandro.lopez@cimav.edu.mx

Introduction

The use of high temperature solid CO_2 capture in several fossil fuel-based energy production processes is an option to improve the efficiencies of such processes and simultaneously reduce the emission of greenhouse gases to the atmosphere. Recent studies in our laboratory [1] have shown the use of Na_2ZrO_3 as an alternate synthetic CO_2 solid sorbent compared to expensive lithium-base sorbents (Li_2ZrO_3 and Li_4SiO_4) [2,3] due to its excellent thermal stability, kinetics and CO_2 capture capacity features. The objective of the present work is to establish the CO_2 sorption kinetics parameters such as: order of reaction, kinetic rate constant, apparent, intrinsic and diffusional activation energies and rate determining step to be used in a further design of a CO_2 sorbent unit.

Experimental

Na_2ZrO_3 was synthesized through the solid state reaction (SS) as described by López-Ortiz et al [4] and Kato et al [5] using stoichiometric amounts of a mixture of Na_2CO_3 and ZrO_2 and calcined for 4 h at 900ºC in an air-heated box furnace according to the following solid state reaction:

$$Na_2CO_3 + ZrO_2 = Na_2ZrO_3 + CO_2 \qquad (1)$$

Afterwards the sample was divided in nine equal portions. Sorption kinetics of prepared samples was evaluated using an electrobalance reactor (TGA) as a function of CO_2 mol fraction (CO_2 partial pressure) and temperature at a flowrate of 150 sccm. These conditions were determined using the CO_2 sorption thermodynamics of Na_2ZrO_3 through thermodynamic calculations using the HSC software [6] and results are presented in Figure 1.

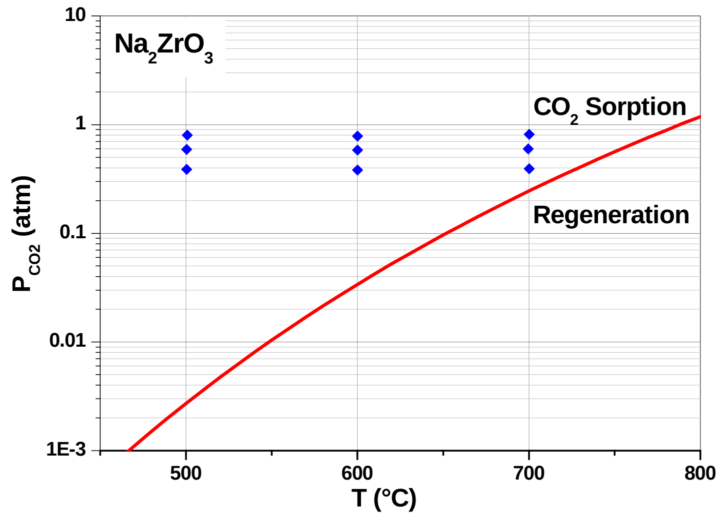

Figure 1. Thermodynamic equilibrium calculations for reaction (1)

From Figure 1 is evident that the nine points used for the kinetic experimental investigation were chosen in the area above the equilibrium line (red line) where the CO_2 sorption by Na_2ZrO_3 is feasible at values of CO_2 partial pressures (P_{CO2}) of less than 1. The area under the equilibrium curve corresponds to the reverse reaction and indicates the region were the sorbent can be regenerated. Therefore, the nine points used for CO_2 sorption were at P_{CO2} = 0.4, 0.6, 0.8 and T = 500, 600, 700ºC.

UHP grade gases were used for all TGA evaluation tests, while about 20 mg of sample were employed on each of the nine tests of the kinetic study. During heating on each test, Ar was introduced as inert and after reaction temperature was reached, a mixture of CO_2/Ar of 150 sccm was accepter to the TGA to start the test. Finally after reaction completion the sample was exposed to an Ar atmosphere again and let to cool down to room temperature. In order to minimize kinetic limitations due to external mass transfer from the gas to the particle and viceversa, the volumetric flowrate employed in the kinetic study was carefully selected by increasing the gas flowrate in the TGA from 100 to 200 sccm until no variation of the reaction rate of a standard test was observed as a function of the volumetric flowrate. Finally, a volumetr4ic flowrate of 150 sccm was selected for all the tests.

Characterization

Characterization of the samples consisted in X-ray diffraction (XRD, Phillips XPERTMPD with CuKα). The BET surface area was measured using a Autosorb 1 from Quantachorome Inc. Morphology of the samples was examined through scanning electronic microscopy (SEM) using a JEOL JSM-5800LV system. Particle size of the synthesized samples was measured through a laser light dispersion technique using a Mastersizer 2000 from Malvern Instruments.

Results and Discussion

Figure 2 shows the XRD diffraction pattern of the synthesized Na_2ZrO_3 at 900ºC. In this Figure it can be observed that the main crystalline phase present in the XRD pattern corresponds to Na_2ZrO_3 with only small traces of unreacted ZrO_2. These small traces of ZrO_2 can be attributed to the inherent nature of the synthesis method employed and is directly related to the limited homogeneity in the reacting mixture.

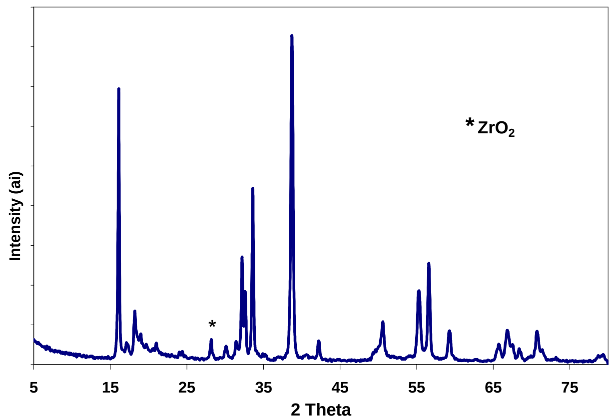

Figure 2. XRD Pattern of the synthesized Na_2ZrO_3 through the SS method

The BET surface area of the synthesized Na_2ZrO_3 resulted in less than 1 m^2/g, which indicates that the CO_2 sorption process will eventually take place through a gas-sold reaction with limited gas diffusion inwards or outwards of the particle.

Results of the particle size distribution of the synthesized Na_2ZrO_3 sample are shown in Figure 3.

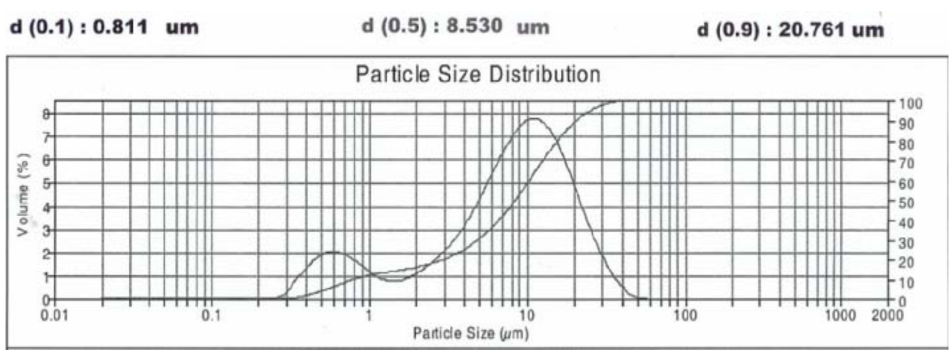

Figure 3. Particle size distribution for the synthesized Na_2ZrO_3 through SS reaction

From this Figure it can bee seen that in the synthesized sample a bimodal particle size distribution is present with peak distributions around 0.6 μm and 10 μm, respectively. The mean distribution particle size was measured to be 8.5 microns.

Morphology of the Na_2ZrO_3 synthesized sample was examined through scanning electron microscopy (SEM). Figure 4 presents two SEM micrographs of the Na_2ZrO_3 sample at different magnifications in the range of 4–2 μm. In this Figure the evidence of the presence of agglomerates of ≈ 8 μm formed from ≈ 1 μm size particles of the CO_2 solid acceptor is confirmed and agrees with the particle size analysis results above described, which indicated a bimodal particle size distribution with large particles of about 10 μm and smaller particles of about 0.6 μm.

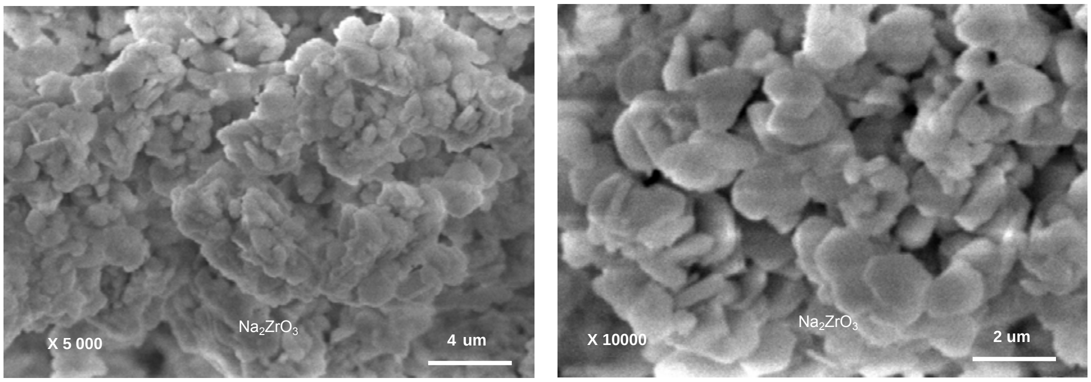

Figure 4. SEM micrographs of synthesized Na_2ZrO_3

Temperature Effect

Figure 5 presents the TGA response plot of dimensionless mass ratio (***M/Mo***) *vs* time (***t***) for reaction (1) at 80% CO_2/Ar and 150sccm. Here in this plot is evident the strong temperature effect as temperature is increased from 500 to 700ºC. The separation of the curves indicates a high dependence of the reaction rate with temperature.

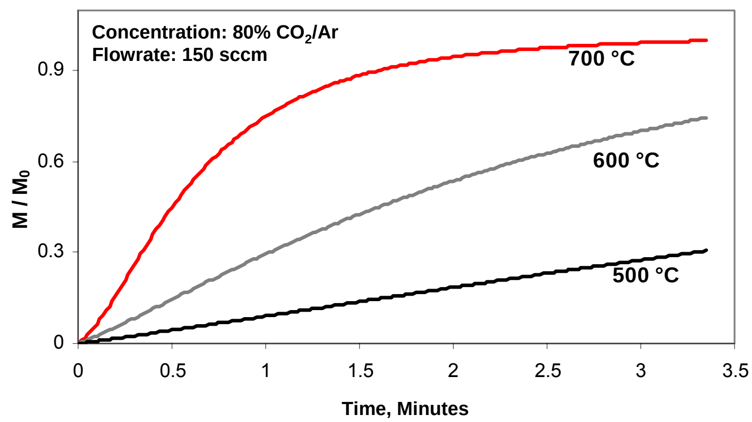

Figure 5. Temperature effect of the CO_2 sorption of Na_2ZrO_3 in the range of 500-700ºC

CO_2 Concentration Effect

Figure 6 shows a TGA response plot of dimensionless mass ratio (***M/Mo***) *vs* time (***t***) for reaction (1) at 600ºC and 40%, 60% and 80% CO_2/Ar and 150sccm. In this plot is observed a strong concentration effect between 40 and 60% CO_2 concentrations. However, the separation of the lines between 60 and 80% CO_2 is not as pronounced as from 40 to 60%. This behavior suggests that possible diffusional limitations within the particles may be important at high values of CO_2 concentrations.

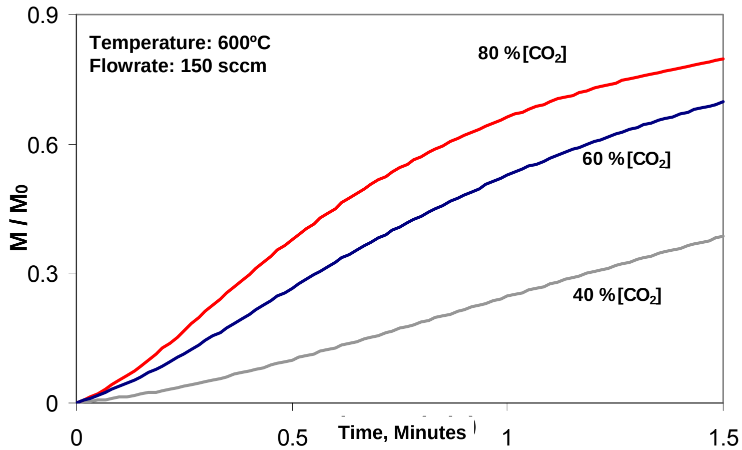

Figure 6. Concentration effect of Na_2ZrO_3 in the range of 40-80% CO_2/Ar

Global Reaction Rate

In a TGA thermogram plot of mass per initial mass (***M/Mo***) versus reaction time (***t***) the initial rate can be reasonably estimated based on the initial lineal region of this plot and this can be assumed to be proportional to the initial reaction rate. This reaction rate was evaluated for each of the nine tests described in the experimental section. Figure 7 shows a sample of the reaction rate calculation of one of the tests at 600ºC and a gas concentration of 60% CO_2/Ar at 150 sccm.

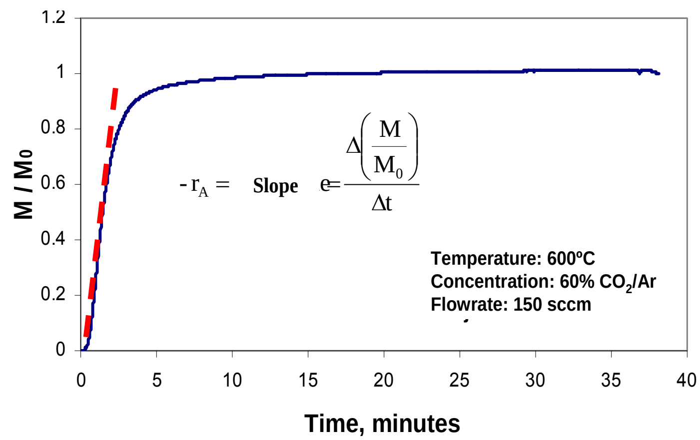

Figure 7. Calculation of the initial reaction rate for the kinetic study

where:

r_A = Initial reaction rate (s^{-1})
Mo = Initial Mass of the sample at the start of the reaction (mg)
M = Mass of the sample during the reaction (mg)
Mf = Mass of the sample after reaction completion (mg)
M/Mo = Mass ratio during the reaction (dimensionless)
t = Reaction time (s)

Also, according to the general rate equation this is equal to the following expression:

$$r_A = kC_A^n \qquad (2)$$

where k is the reaction rate constant, C_A is the CO_2 concentration in mol fraction, and n is the reaction order with respect to C_A.

Figure 7 shows the reaction order calculation with respect to CO_2 concentration evaluated under the conditions described in the experimental section. The reaction order varies from 1.12 at 500ºC to 1.16 at 600ºC to 1.14 for 700ºC and the average of these values results in a reaction order of 1.1. Correlation coefficients of the linear regressions for each temperature were approximately of 1, which confirms a global reaction rate order of 1 with respect to CO_2 concentration. Therefore, the reaction order of the referenced reaction (1) was assumed to be of 1.

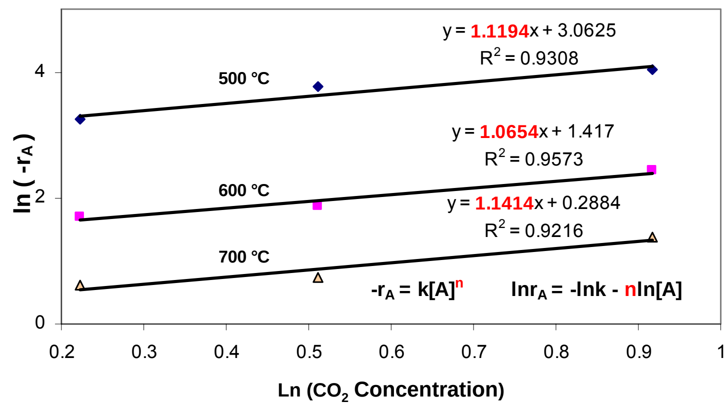

Figure 8. Calculation of the global reaction rate order

Figure 9 shows a plot of - $\boldsymbol{r_A}$ *vs* % CO_2 concentration for the calculation of the reaction constant (k) of equation (2). In this plot a strong temperature effect is observed and agrees with results presented previously in Figure 5. In Figure 9 the separation of the lines and the increase in k values calculated through linear regression confirm this effect.

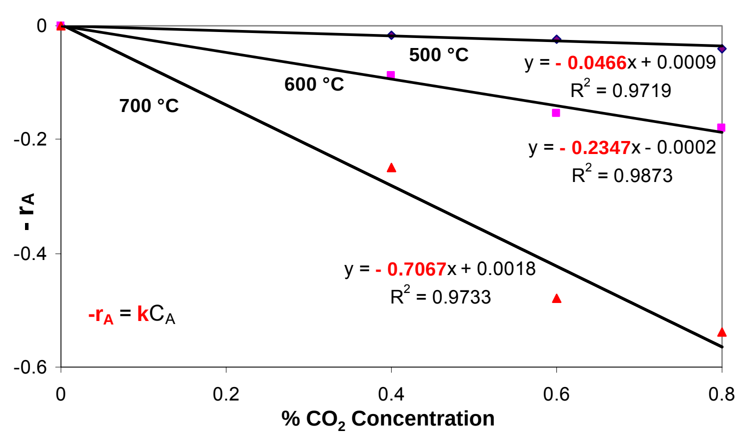

Figure 9. Calculation of the global reaction rate constant

Finally, Figure 10 presents an Arrhenius plot of the calculated global kinetic parameters for the CO_2 sorption of Na_2ZrO_3.

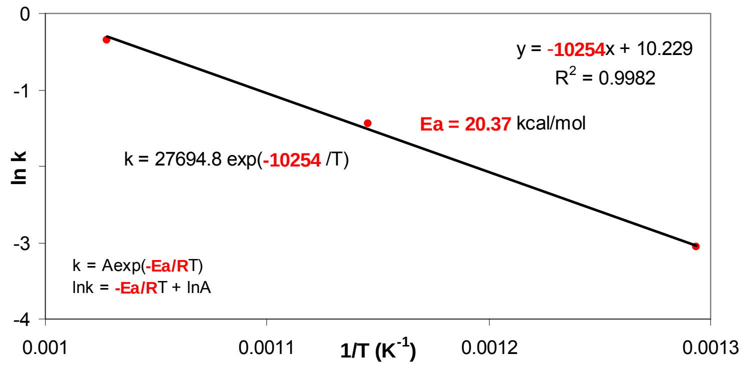

Figure 10. Arrhenius of the global reaction rate for the CO_2 sorption of Na_2ZrO_3

Calculated apparent activation energy obtained for the CO_2 sorption of Na_2ZrO_3 resulted in 20.4 Kcal/mol (Figure 10). This high apparent activation energy suggests that the overall reaction rate is controlled by the chemical reaction resistance, since its value is approximately greater that 20 Kcal/mol, which is characteristic of chemically controlled reactions [7]. Therefore, equation (2) can be expressed in terms of known global rate parameters as follows:

$$-r_A = 27694.8 \exp\left(-20.37 / RT\right) y_{CO_2} \quad (3)$$

where r_{CO2} has units of (s^{-1}), the activation energy has units of (E_A = 20.37) Kcal/mol, y_{CO2} is given in molar fraction, R = 1.987E^{-3} Kcal/mol K, and T = K.

Reaction Modeling

The approximate solution to the shrinking core model [8] was chosen to model the experimental time conversion-results, While the rigorous model requires a numerical solution, the approximate model solution is algebraic and provides a satisfactory representation of the exact solution. Using the symbols of Levenspiel et al. [8], the time-fractional conversion relationship is given by

$$t = \frac{1}{S_m} X + \frac{1}{S_g}\left[1 - 3(1-X)^{2/3} + 2(1-X)\right] + \frac{1}{S_r}\left[1-(1-X)^{1/3}\right] \quad (4)$$

where the terms on the right hand side represent the chemical reaction resistance (*Sr*), product layer diffusion resistance (*Sg*) and external mass transfer resistance (*Sm*), which control the reaction in the particle. Therefore, the time required to achieve a specific fractional conversion is approximated as the sum of the times associated with the individual resistances.

In equation (4) fractional conversion was calculated according the following expression:

$$X = \frac{1-\left(\frac{M}{M_0}\right)}{1-\left(\frac{M_f}{M_0}\right)} \quad (5)$$

Although the reaction is exothermic, the isothermal analysis is justified based on the small mass of solid reactant. According to Lopez Ortiz et al. [9] a temperature increase of about 25ºC would exist only momentarily near the beginning of the reaction in their TGA modeling studies of FeS oxidation with O_2.

In equation (4) all the resistance coefficients are determined by the following expressions:

$$S_m = \frac{3C_A k_g}{aRC_{S0}} = \frac{bkm_A C_{A0}}{\tau(1-\varepsilon)\rho_s} \quad (6)$$

$$S_g = \frac{6D'_{eA}C_A}{aR^2 C_{S0}} = \frac{6bD_g C_{A0}}{r^2 \rho_s} \quad (7)$$

$$S_r = \frac{bk_s C_A}{R} = \frac{bk_s C_{A0}}{r\rho_s} \quad (8)$$

where km_A represents the volumetric mass transfer coefficient between bulk gas and solid exterior surface (cm^3/s), b is the stoichiometric coefficient, ratio of mols of solid reactant per mol gaseous reactant that according to reaction (9) takes a value of 1

$$Na_2ZrO_3 + CO_2 = Na_2CO_3 + ZrO_2 \quad (9)$$

τ is the thickness of the particle (cm), C_{Ao} is the bulk reactant concentration of reactant gas (mol/cm^3), ε is the void fraction of the solid reactant particle, ρ_s is the solid molar density (mol/cm^3), k_g is the reaction rate constant for the gaseous species (cm^3/s), a is the number of mols of gas (denoted as A) reacting with one mol of solid (denoted as S), R is the average diameter of the solid particle (cm), C_{So} is referred as the concentration of the solid particle (mol), D'_{eA} is the effective diffusion coefficient of the gas (cm^2/s), D_g is the product layer diffusion coefficient between grains (cm^2/s), r is the transient radius of the particle (cm), and finally k_S is referred as the reaction rate constant for the solid (cm^3/s). For details of calculation of these parameters the reader can be referred to Lopez Ortiz [10] and Barraza [11].

From equation (4) and experimental curves of *X vs t* for the CO_2 sorption of Na_2ZrO_3 reaction (9) best fitting coefficients *Sr*, *Sg* and *Sm* were determined for each experimental run. Based on the fitting results, the mass transfer resistance (*Sm*) resulted in almost negligible values compared to those for *Sr* and *Sg*. This last behavior was expected since prior to the beginning of the TGA experiments a feed gas flowrate was determined (150 sccm) in order to minimize external mass transfer effects on the reacting sample.

Table 1 shows results of best fitting values to equation (4) for each of the runs performed in the experimental section of this work.

Table 1. Results of best fitted values of Sr and Sg against experimental data

Temperature (° C)	$[CO_2]$ (%)	S_r (s^{-1})	S_g (s^{-1})
500	40	0.051	0.556
500	60	0.057	0.894
500	80	0.082	1.396
600	40	0.179	0.875
600	60	0.326	1.496
600	80	0.554	1.767
700	40	0.555	1.283
700	60	1.532	2.364
700	80	1.758	2.524

Also, Table 2 presents calculated values for the solid surface reaction constant (k_S) and the product layer diffusion coefficient (D_g) based on results of Table 1.

Table 2. Calculated vales of k_s and D_g for the modeling work

Temperature (°C)	$[CO_2]$ (%)	$k_s \times 10^{-2}$ (cm^3/mol*s*cm^2)	$D_g \times 10^{-5}$ (cm^2/s)
500	40	8.8	6.8
600	40	35.1	12.2
700	40	121.0	19.9
500	60	6.6	7.3
600	60	42.5	13.9
700	60	222.7	24.4
500	80	7.1	8.6
600	80	54.2	12.3
700	80	191.6	19.5

From results of Table 2 it is observed that as temperature increases the value of the intrinsic surface reaction rate constant, k_S, also increases and independently from the CO_2 concentration. This behavior was expected since a strong temperature effect was observed in the TGA response plots of Figure 5. However, no significant change in the diffusion coefficient values are observed as temperature increases for the same CO_2 concentration. This last behavior agrees well with theory that temperature effect in the diffusion coefficient is relatively small compared to the effect that temperature has in the rate reaction constant.

Also these results provide a clear view of the behavior that is expected in terms of the contributions of the corresponding resistances with respect to temperature, since *Sr* is directly proportional to k_S (see equation 8) and also inversely proportional to reaction time ***t***. It is expected that as temperature increases the contribution of the chemical reaction resistance to the total time is reduced compared to contributions at lower temperatures. Therefore it can be concluded that the contribution of the chemical reaction resistance is strongly affected by the temperature and only mildly by the CO_2

concentration. In the case of the gas diffusion coefficient, due to the fact that a small change is expected from an increase in reaction temperature its contribution to the total time will remain at a constant CO_2 concentration.

The physical meaning of these coefficients is related to a combination of chemical reaction and diffusion through the product layer processes, which dominate the reaction rate of CO_2 sorption of Na_2ZrO_3.

Once the intrinsic rate constant values (k_S) from Table 2 were calculated the intrinsic activation energy can be also calculated from the Arrhenius expression and this is presented in Figure 11.

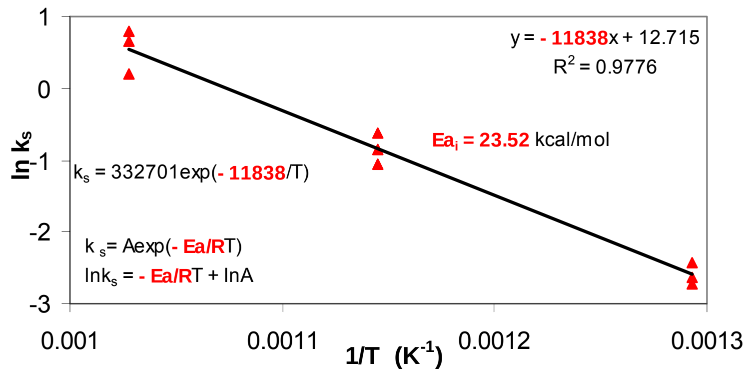

Figure 11. Arrhenius plot of intrinsic activation energy calculation

From Figure 11 the observed value of intrinsic activation energy for the CO_2 sorption of Na_2ZrO_3 was 20.37 Kcal/mol, which suggest that the sorption kinetics are controlled by the chemical reaction process.

If is assumed that an Arrhenius-type proportionality exists between Dg and temperature, the diffusional Arrhenius type activation energy can also be calculated from the data of Table 2. Figure 12 shows the Arrhenius-type gas diffusional activation energy calculated for the CO_2 sorption of Na_2ZrO_3.

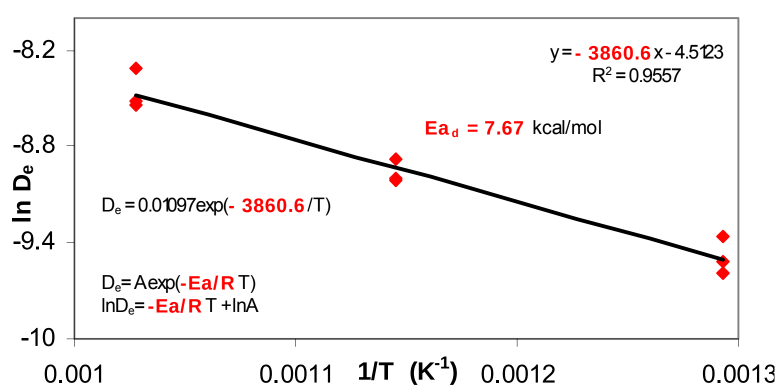

Figure 12. Arrhenius plot of diffusional activation energy calculation

Figure 11 it is evident that Dg values are well represented in terms of an Arrhenius type equation. For a kinetic process to be considered with small diffusional limitations the Arrhenius-type diffusional activation energy should be less than ≈ 20 Kcal/mol [7]. If not, this diffusional process is expected to significantly influence in the apparent activation energy and consequently in the overall rate of the process. However, the calculated value observed in Figure 11 is of only 7.67 Kcal/mol and therefore this value suggests that gas diffusional limitations through the product layer are expected not to be determinant in the overall reaction rate since this value is well below the reference value of 20 Kcal/mol. Otherwise, modification of the solid particle size to adjust or minimize diffusional limitations would be needed.

Once the both resistances were determined the overall time dependent conversion equation was defined as follows:

$$t_{total} = \frac{1}{3\times10^{10} C_A \exp(-23522/RT)}\left[1-(1-X)^{1/3}\right] + \frac{1}{1.4\times10^{7} C_A \exp(-7671/RT)}\left[1-3(1-X)^{2/3}+2(1-X)\right] \quad (10)$$

Figure 13 shows the plot of one of the runs at 700ºC and 80% CO_2/Ar at 150 sccm of experimental values against the resulted model equation (10). As can be observed in this plot a good fitting results between experimental values and the model.

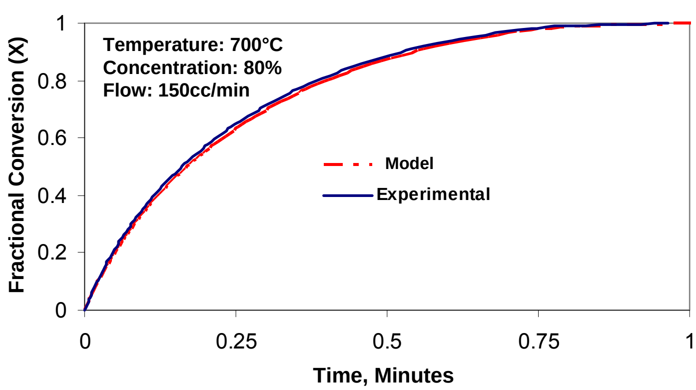

Figure 13. Comparison between model results and experimental values

Equation (10) indicates that a two-resistance process controls the overall kinetics. However, the final question in this modeling effort was to determine which of these resistances is considered as the rate determining step (RDS) of the reaction kinetics.

In order to clarify this issue the variation of each relative (chemical + diffusional) resistance with respect to fractional conversion was calculated for each experimental run. As a result, most of the runs presented a behavior that at the beginning of each run about 99% of the resistance is regarded to the chemical reaction with almost negligible contribution of the diffusional resistance. However, towards the end of each run approximately, 63% of the contribution is regarded to the chemical reaction resistance, while the remaining 37% is attributed to the gas diffusion resistance through the product layer.

Conclusions

The global rate of the CO_2 sorption reaction by the Na_2ZrO_3 was of first order in CO_2 and strongly dependent on temperature. The calculated apparent activation energy was E_A = 20.4 kcal/mol. Data analysis used the approximate solution to the shrinking core model for a gas-solid reaction. A two resistance (surface reaction and product layer diffusion) kinetic variation of the model provides good match with the conversion-time data. Modeling results include; an intrinsic activation energy of 23.5 kcal/mol and a product layer diffusional activation energy of 7.7 kcal/mol. The dependence of the reaction coefficients on reaction variables was in general in agreement with theory. Finally, results indicate that the main resistance to the reaction rate is the surface reaction, which is controlling the reaction kinetics (rate determining step) with only a minor contribution of the product layer diffusion resistance towards the end of the reaction.

Acknowledgements

This research was supported by Consejo Nacional de Ciencia y Tecnología (CONACYT-México) and Centro de Investigación en Materiales Avanzados (CIMAV) under contract 40118-Y. The help and advice provided by Enrique Torres in the XRD analysis of the samples is greatly appreciated.

References

[1] López Ortiz A., Pérez Rivera N. G., Reyes Rojas A., Lardizábal Gutiérrez D. Sep. Sci. Tec. 39 (2004) 3559.
[2] Nakagawa, K; Ohashi, T. J., J. Electrochem. Soc., 145 (1998) 1344
[3] Kato, M.; Yoshikawa, S.; Essaki, K.; Nakagawa, K. In Toshiba Corporation. INTERMAC, 2001, Japan Electric Measuring Instruments Manufacturers' Association, Joint Technical Conference, Paper ID: SE-3 (1021).
[4] López Ortiz A., Pérez Rivera N. G., Reyes Rojas A., Lardizábal Gutiérrez D., Sep. Sci. Technol., 2004, Vol. 39, No. 15, 356
[5] M. Kato, S. Yoshikawa, K. Nakagawa., J. Mater. Sci. Lett. 21, 2002, 485.
[6] Roine A., “Chemical reaction and equilibrium software with extensive thermochemical database”, Outokumpu HSC 5.11 Chemistry for windows, (2002).
[7] G. F. Froment and K.B. Bischoff (1990), Chemical Reaction Analysis and Design, 2nd edn. Jhon Wiley & Sons, New York.
[8] A. Lopez Ortiz, F. R. Groves and D. P. Harrison. Chemical Engineering Communications, Vol. 177, pp65-85, 2000.
[9] O. Levespiel, (1972), Chemical Reaction Engineering, 2nd edn., Jhon Wiley & Sons, New York.
[10] A. Lopez Ortiz, “Kinetic Study of the Regeneration of Iron Sulfide (FeS)” Master Degree Thesis Louisiana State University, Chemical Engineering Department Baton Rouge, Louisiana, 1996.
[11] D. Barraza, “Método de Síntesis Alterno Estudio Cinético y Modelación de la Absorción de CO_2 por el Na_2ZrO_3” Master Degree Thesis, Materials Science Department, Research Center for Advanced Materals (CIMAV), Chihuahua, Chihuahua, Mexico, July 2005 .